Numerical investigation of orthotropic finite elasticity problem with discontinuous deformation gradient

Adair R. Aguiar[1], Lucas A. Rocha[1]

[1]*Department of Structural Engineering, São Carlos School of Engineering, University of São Paulo*
Av. Trabalhador Sãocarlense, 400, Cx. P. 359, 13560-590, São Carlos-SP, Brazil
aguiarar@sc.usp.br, lucas.almeida.rocha@usp.br

Abstract. We consider the problem of an elastic annular disk in equilibrium in the absence of body force. The disk is fixed on its inner surface and compressed by a uniform pressure on its outer surface. The disk is made of a cylindrically orthotropic material that is stiffer in the radial direction than in the tangential direction. Such material properties are found in certain types of wood and carbon fibers with radial microstructure. We consider that the disk is made of a cylindrically orthotropic St Venant-Kirchhoff material, which is a natural constitutive extension from the linear to the nonlinear elasticity theory. The solution of this problem predicts material overlapping, which is unphysical if either the pressure is large enough or the inner radius is small enough. A way to prevent this anomalous behavior consists of imposing the local injectivity constraint through a constrained minimization problem of the energy functional. We use both a penalty and an augmented Lagrangian formulation to obtain convergent sequences of finite element approximations. Our results indicate that, to impose the local injectivity constraint accurately, it is preferable to increase the degree of the finite element approximation than to increase the number of finite elements in the mesh.

Keywords: Nonlinear elasticity, Orthotropy, Constrained Minimization, Non-smooth deformation, Finite element method

1 Introduction

We consider the problem of an elastic annular disk with uniform thickness in equilibrium in the absence of body force. The disk is fixed on its inner surface of radius $R_i > 0$ and compressed by a uniform pressure $p > 0$ on its outer surface of radius $R_e > R_i$. The disk is made of a cylindrically orthotropic material that has a constitutive response that is stiffer in the radial direction than in the tangential direction. Material properties of this type are found in certain types of woods, carbon fibers with radial microstructure, and fiber-reinforced composites [1–3].

In the context of the classical linear elasticity theory, the solution of this problem predicts material overlapping for a large enough pressure, which is not physically acceptable. In addition, material overlapping is associated with large strains, which violate the hypothesis of infinitesimal strains upon which the linear elasticity theory is based. A natural constitutive extension of the linear to the nonlinear elasticity theory consists of considering that the disk is made of an orthotropic St Venant-Kirchhoff material. In this case, there is a pressure above which the solution of the corresponding nonlinear disk problem predicts material overlapping in an interior region of the disk. In addition, there is a jump in the deformation gradient across an interior surface of the disk [4].

Fosdick and Royer-Carfagni [5] have proposed a theoretical approach to eliminate the anomalous behavior of material overlapping in classical linear elasticity. The approach consists of minimizing the total potential energy functional subject to the condition that the determinant of the deformation gradient be not less than a small positive parameter.

In this work, we extend this investigation to the nonlinear elasticity theory by considering the problem of minimizing the total potential energy functional of a nonlinear disk subject to the local injectivity constraint. We use both a penalty and an augmented Lagrangian formulation to obtain convergent sequences of numerical solutions that do not predict material overlapping and that correspond to non-smooth deformation fields. Analogous fields were also reported by Aguiar and Rocha [4] in the study of the unconstrained nonlinear case.

In Section 2, we formulate the disk problem as the minimization of the total potential energy functional subjected to the local injectivity constraint. In Section 3, we consider a numerical example and present converging results using both a penalty and an augmented Lagrangian formulation. In addition, we compare how accurately each formulation imposes the local injectivity constraint. In Section 4, we present some concluding remarks.

2 The disk problem

Let $\mathcal{B} \subset \mathbb{R}^3$ denote the undistorted reference configuration of a homogeneous hyperelastic solid in equilibrium. Points $\mathbf{x} \in \mathcal{B}$ are mapped into points $\mathbf{y} \triangleq \mathbf{f}(\mathbf{x}) = \mathbf{x} + \mathbf{u}(\mathbf{x})$, where $\mathbf{f}$ and $\mathbf{u}$ are the deformation and the displacement fields, respectively. The boundary $\partial\mathcal{B}$ of $\mathcal{B}$ is composed of two non-intersecting parts, $\partial_1\mathcal{B}$ and $\partial_2\mathcal{B}$, $\partial\mathcal{B} = \partial_1\mathcal{B} \cup \partial_2\mathcal{B}$, $\partial_1\mathcal{B} \cap \partial_2\mathcal{B} = \emptyset$, such that $\mathbf{f} = \bar{\mathbf{f}}$ on $\partial_1\mathcal{B}$, where $\bar{\mathbf{f}}$ is a given function, and the traction field $\bar{\mathbf{t}}$ is applied on $\partial_2\mathcal{B}$. In this work, $\bar{\mathbf{t}}$ is a pressure load, which is constant in the deformed configuration and given by $\bar{\mathbf{t}} = -p \operatorname{cof} \mathbf{F}\, \mathbf{N}$, where $p > 0$, $\operatorname{cof} \mathbf{F} \triangleq (\det \mathbf{F})\, \mathbf{F}^{-T}$, $\mathbf{N}$ is the outward unit normal to $\partial_2\mathcal{B}$, and $\mathbf{F} \triangleq \nabla\mathbf{f} = \mathbf{I} + \nabla\mathbf{u}$, with ∇ denoting the gradient operator with respect to $\mathbf{x}$ and $\mathbf{I}$ denoting the identity tensor.

We consider the minimization of the total potential energy functional given by [6]

$$\min_{\mathbf{f} \in \mathcal{A}_\varepsilon} \mathcal{E}(\mathbf{f})\,, \qquad \mathcal{E}(\mathbf{f}) = \int_{\mathcal{B}} W(\mathbf{F})\, \mathrm{d}\mathbf{x} + \frac{p}{3} \int_{\partial\mathcal{B}} (\operatorname{cof} \mathbf{F}\, \mathbf{N}) \cdot \mathbf{f}\, \mathrm{d}\mathbf{x}\,, \tag{1}$$

where $\mathcal{A}_\varepsilon$ is the set of kinematically admissible deformation fields, such that $\det \mathbf{F} \geq \varepsilon > 0$ in $\mathcal{B}$ and $\mathbf{f} = \bar{\mathbf{f}}$ on $\partial_1\mathcal{B}$, ε is a small positive parameter, and W is the strain energy density function.

In this work, $\mathcal{B}$ is an annular disk with inner radius $R_i > 0$, outer radius $R_e > R_i$, and unitary thickness. In addition, $\partial_1\mathcal{B}$ and $\partial_2\mathcal{B}$ are the inner and outer surfaces of the disk, respectively, $\bar{\mathbf{f}} = \mathbf{x}$, which means that the disk is fixed on its inner surface, and p is a uniform pressure acting on the outer surface.

The disk is made of a cylindrically orthotropic St Venant-Kirchhoff material so that

$$W = \frac{1}{2}\, \mathbf{E} \cdot \mathbb{C}[\mathbf{E}]\,, \qquad \mathbf{E} \triangleq \frac{1}{2}\, (\mathbf{F}^T \mathbf{F} - \mathbf{I})\,, \tag{2}$$

where $\mathbb{C}$ is the elasticity tensor, with the nonzero components c_{11}, c_{22}, c_{33}, c_{12}, c_{13}, c_{23}, c_{44}, c_{55}, c_{66}; see, for instance, Daniel and Ishai [3].

Let $\{\mathbf{e}_R, \mathbf{e}_\Theta, \mathbf{e}_Z\}$ denote the usual orthonormal cylindrical basis at $\mathbf{x}$ associated with the cylindrical coordinates (R, Θ, Z), such that $\mathbf{x} = R\, \mathbf{e}_R(\Theta) + Z\, \mathbf{e}_Z$. Similarly, let $\{\mathbf{e}_r, \mathbf{e}_\theta, \mathbf{e}_z\}$ and (r, θ, z) be the corresponding orthonormal cylindrical basis and coordinates, respectively, at $\mathbf{y}$, such that $\mathbf{y} = r\, \mathbf{e}_r(\theta) + z\, \mathbf{e}_z$. Unless stated otherwise, we shall omit the dependence of $\mathbf{e}_R$ and $\mathbf{e}_r$ on Θ and θ, respectively.

We want to find a deformation field $\mathbf{f}$, such that points $\mathbf{x} = (R, \Theta, Z) \in [R_i, R_e] \times [0, 2\pi] \times [0, 1]$ move along radial lines according to

$$\mathbf{f}(R, \Theta, Z) = r(R)\, \mathbf{e}_r(\Theta) + Z\, \mathbf{e}_z\,, \tag{3}$$

which corresponds to a displacement field with the form

$$\mathbf{u}(R, \Theta, Z) = u_r(R)\, \mathbf{e}_R\,, \qquad u_r(R) = r(R) - R\,. \tag{4}$$

Since $\mathbf{F} \triangleq \nabla\mathbf{f}$, we have that

$$\mathbf{F} = \nu(R)\, \mathbf{e}_r \otimes \mathbf{e}_R + \tau(R)\, \mathbf{e}_\theta \otimes \mathbf{e}_\Theta + \mathbf{e}_z \otimes \mathbf{e}_Z\,, \qquad \nu(R) \triangleq r'(R)\,, \quad \tau(R) \triangleq r(R)/R\,, \tag{5}$$

where the explicit dependence on $\mathbf{x} = (R, \Theta, Z)$ is omitted and $(\cdot)'$ denotes the derivative with respect to R.

It follows from eq. (1.b), eq. (2), eq. (4.b), and eq. (5) that the total potential energy functional $\mathcal{E}$ can be written as

$$\begin{aligned} \mathcal{E} = \pi \int_{R_i}^{R_e} \Big(&\frac{c_{11}}{4}\, R\, {u_r'}^4 + c_{11}\, R\, {u_r'}^3 + c_{11}\, R\, {u_r'}^2 + c_{12}\, u_r\, {u_r'}^2 + 2\, c_{12}\, u_r\, u_r' + \frac{c_{12}}{2\, R}\, u_r^2\, {u_r'}^2 + \frac{c_{12}}{R}\, u_r^2\, u_r' \\ &+ \frac{c_{22}}{R}\, u_r^2 + \frac{c_{22}}{R^2}\, u_r^3 + \frac{c_{22}}{4\, R^3}\, u_r^4 \Big)\, \mathrm{d}R + \pi\, p\, \left[(R_e + u_r(R_e))^2 - R_i^2 \right], \end{aligned} \tag{6}$$

where we have used the boundary condition $u_r(R_i) = 0$. Note from eq. (6) that, even though the material is orthotropic, the total potential energy functional depends only on the elastic moduli c_{11}, c_{22}, and c_{12}.

3 Numerical procedure and results

We consider a Finite Element formulation of the minimization problem given by eq. (1.a) and eq. (6), where the displacement field $\mathbf{u}$, which has the form given by eq. (4), is the unknown variable. Let $\mathcal{V}_h$ be a finite dimensional space spanned by a set of basis functions $\{\mathbf{w}_i\}$, where h stands for the characteristic length of the finite element. Then, an approximate minimizer $\mathbf{u}_h \in \mathcal{V}_h$ can be written as

$$\mathbf{u}_h = \sum_{i=1}^{m} s_i \, \mathbf{w}_i \,, \tag{7}$$

where $s_i \in \mathbb{R}$, $i = 1, 2, 3, ..., m$, is a degree of freedom and m is the number of degrees of freedom associated with the discretization. In this work, we use Lagrange finite elements of degree d and a Gauss-Legendre quadrature rule with $2\,d$ points.

It follows from eq. (2) and eq. (5) that the radial normal stress $P_{rr} \triangleq \mathbf{e}_r \cdot \mathbf{P}\,\mathbf{e}_R$, where $\mathbf{P} = \partial W/\partial \mathbf{F}$ is the first Piola-Kirchhoff stress tensor, is given by

$$P_{rr}(R) = \hat{P}_{rr}(\tau, \nu) \triangleq \left[c_{11}\,(\nu^2 - 1) + c_{12}\,(\tau^2 - 1)\right] \nu/2 \,. \tag{8}$$

It is possible to verify that, for $|\tau| < \sqrt{1 + c_{11}/c_{12}}$, $\hat{P}_{rr}$ is non-monotonic with respect to ν. Its inflection points occur at $\nu = \nu^{\,\mathrm{inf}}$ and $\nu = -\nu^{\,\mathrm{inf}}$, where

$$\nu^{\,\mathrm{inf}} \triangleq \frac{\sqrt{3}}{3} \sqrt{\frac{-\tau^2\,c_{12} + c_{11} + c_{12}}{c_{11}}} \,. \tag{9}$$

Aguiar and Rocha [4] have considered the minimization problem given by eq. (1.a) and eq. (6) without imposing the local injectivity constraint $\det \mathbf{F} \geq \varepsilon > 0$. The authors have observed that there is a value of pressure $\bar{p}$, below which we find smooth minimizers such that $\nu(R) > \nu^{\,\mathrm{inf}}$ and $\det \mathbf{F} > 0$ in the whole disk. For $p > \bar{p}$, the authors have found minimizers that are non-smooth at $R = R_{\mathcal{S}}$; furthermore, $\nu(R) < -\nu^{\,\mathrm{inf}} < 0$ for $R \in [R_i, R_{\mathcal{S}})$ and $\nu(R) > \nu^{\,\mathrm{inf}} > 0$ for $R \in (R_{\mathcal{S}}, R_e]$. These non-smooth minimizers were found by using a numerical procedure that introduces $R_{\mathcal{S}}$ as an additional variable of the problem. Here, we use a similar procedure. We assume that the local injectivity constraint is active in $R \in (R_i, R_{\mathcal{S}})$ and then we search for the value of $R_{\mathcal{S}}$ that minimizes the total potential energy functional.

We impose the local injectivity constraint using both a penalty and an augmented Lagrangian formulation. For that, we introduce the functionals

$$\mathcal{P}(\mathbf{u}, R_{\mathcal{S}}) \triangleq \frac{\delta}{2} \int_{\mathcal{B}_=} c^2 \,\mathrm{d}\mathbf{x} + \delta^{\,\mathrm{inf}} \int_{\mathcal{B}_>} \max\left(0, \nu^{\,\mathrm{inf}} - \nu\right)^2 \mathrm{d}\mathbf{x} \,, \tag{10}$$

$$\mathcal{L}(\mathbf{u}, R_{\mathcal{S}}) \triangleq \int_{\mathcal{B}_=} \left(-\lambda\, c + \frac{\delta}{2}\, c^2\right) \mathrm{d}\mathbf{x} + \delta^{\,\mathrm{inf}} \int_{\mathcal{B}_>} \max\left(0, \nu^{\,\mathrm{inf}} - \nu\right)^2 \mathrm{d}\mathbf{x} \,, \tag{11}$$

where $\lambda = \lambda(R)$ is the Lagrange multiplier field associated with the constraint $c \triangleq \det \mathbf{F} - \varepsilon = 0$ in $\mathcal{B}_=$, $\delta > 0$ and $\delta^{\,\mathrm{inf}} > 0$ are penalty parameters, $\mathcal{B}_= = \{\mathbf{x} \in \mathcal{B} \,|\, R_i < R < R_{\mathcal{S}}\}$, and $\mathcal{B}_> = \{\mathbf{x} \in \mathcal{B} \,|\, R_{\mathcal{S}} < R < R_e\}$. The functionals $\mathcal{P}$ and $\mathcal{L}$ are similar to the penalty functional used by Aguiar and Rocha [4], who have considered the minimization problem given by (1.a) and eq. (6) without imposing the constraint $\det \mathbf{F} \geq \varepsilon$. Here, however, the integrals in $\mathcal{B}_=$ have a different form because we impose $\det \mathbf{F} > \varepsilon$. In addition, note that $R_{\mathcal{S}}$ is not limited to be in the interval $[R_i, R_e]$; for instance, $R_{\mathcal{S}} < R_i$ means that $\mathcal{B}_= = \emptyset$ and $\mathcal{B}_> = \mathcal{B}$, that is, the constraint is not active anywhere in the disk. This is the expected behavior when p is small enough.

The discrete version of the minimization problem given by eq. (1.a) and eq. (6) can be written as

$$\min_{R_{\mathcal{S}} \in \mathbb{R}} \; \min_{\mathbf{s} \in \mathbb{R}^m} \mathcal{F}(\mathbf{s}, R_{\mathcal{S}}) \,, \qquad \mathcal{F}(\mathbf{s}, R_{\mathcal{S}}) = \begin{cases} \mathcal{E}_h(\mathbf{s}) + \mathcal{P}_h(\mathbf{s}, R_{\mathcal{S}}) & \text{(Penalty formulation)} \\ \mathcal{E}_h(\mathbf{s}) + \mathcal{L}_h(\mathbf{s}, R_{\mathcal{S}}) & \text{(Augmented Lagrangian formulation)} \end{cases} , \tag{12}$$

where we have used eq. (7) to introduce the vector $\mathbf{s} \triangleq (s_1, s_2, ..., s_m)$ and the functions $\mathcal{E}_h(\mathbf{s}) \triangleq \mathcal{E}(\mathbf{x} + \mathbf{u}_h)$, $\mathcal{P}_h(\mathbf{s}, R_{\mathcal{S}}) \triangleq \mathcal{P}(\mathbf{u}_h, R_{\mathcal{S}})$, and $\mathcal{L}_h(\mathbf{s}, R_{\mathcal{S}}) \triangleq \mathcal{L}(\mathbf{u}_h, R_{\mathcal{S}})$. The lower-level problem is a minimization problem in the vector variable $\mathbf{s}$ parameterized by $R_{\mathcal{S}}$. The upper-level problem is a minimization problem in the scalar variable $R_{\mathcal{S}}$, which we solve by using the golden-section search. See, for instance, Luenberger and Ye [7].

We set the initial search interval of the golden-section search to be $[0.9\,R_i, 0.02\,R_e]$. At each iteration of this method, we solve the lower-level minimization problem for a given $R_{\mathcal{S}}$ using a standard numerical procedure,

which we comment more below. Then, we evaluate the corresponding $\mathcal{F}(\mathbf{s}, R_{\mathcal{S}})$ and proceed to the next iteration, where the search interval is reduced. We repeat these iterations until the search interval is smaller than a certain tolerance, which is equal to 10^{-6} in this work.

For both penalty and augmented Lagrangian formulations, we use $\nu^{\inf} = 1000$ as it was done by Aguiar and Rocha [4]. For the penalty formulation, we use increasingly larger values of δ. Starting from $\delta = \delta_0$ and $\mathbf{s} = \mathbf{s}_0$, we solve the lower-level problem using a standard Newton-Raphson method with a unidirectional search. Then, we increase δ and solve again the lower-level problem starting from the solution of the previous one. We repeat this process until $\delta = \delta_f^p$, where the value of δ_f^p is given below. In this formulation, the numerical approximation of λ is obtained in a post-processing calculation as $\lambda = -\delta\, c$.

For the augmented Lagrangian formulation, we use a constant value $\delta = \delta_f^a$, where the value of δ_f^a is given below. In addition, we introduce a finite element approximation of λ given by

$$\lambda_h = \sum_{i=1}^{m_\lambda} l_i\, w_i\,, \tag{13}$$

where $l_i \in \mathbb{R}$, $i = 1, 2, 3, ..., m_\lambda$, is a degree of freedom, m_λ is the number of degrees of freedom associated with the approximation of λ, and w_i is a shape function of the finite element approximation. In this work, λ_h is constant by parts, so m_λ coincides with the number of mesh elements used in the discretization. Starting from $l_1 = l_2 = ... = l_{m_\lambda} = 0$ and $\mathbf{s} = \mathbf{s}_0$, we solve the lower-level minimization problem using a standard Newton-Raphson method with a unidirectional search. Then, we update l_i, $i = 1, 2, 3, ..., m_\lambda$, as explained below and solve again the lower-level problem starting from the solution of the previous problem. We repeat this process until the update of λ_h is lower than a certain tolerance. We update l_i, $i = 1, 2, 3, ..., m_\lambda$, using the following recursive formula.

$$l_i^{(k+1)} = l_i^{(k)} - \delta\, c_i^{(k)}\,, \tag{14}$$

where the superscript denotes an iteration and $c_i^{(k)}$ is equal to c evaluated at the center of the i-th mesh element in the k-th iteration. For more details on the Newton-Raphson method, the unidirectional search, and the augmented Lagrangian method mentioned above, see, for instance, Luenberger and Ye [7].

We now consider the engineering constants $E_1 = 15$, $E_2 = E_3 = 1$, $\mathrm{v}_{12} = \mathrm{v}_{13} = 0.25, \mathrm{v}_{23} = 0.5$, where E and v denote the Young's modulus and the Poisson ratio, respectively, and the subscripts 1, 2, and 3 denote the radial, tangential, and axial directions, respectively. The values of E_1, E_2, and E_3 multiplied by a factor of 10^{10} are, approximately, the constants of a unidirectional carbon/epoxy composite [3]. These engineering constants correspond to the elasticity constants

$$c_{11} = 900/59 \approx 15.2542\,, \qquad c_{12} = 30/59 \approx 0.508475\,, \qquad c_{22} = 239/177 \approx 1.35028\,. \tag{15}$$

To obtain the numerical results presented below, we use non-uniform meshes parameterized by $q \in \mathbb{N}$ and composed of $N = 24 \times 2^q$ elements distributed in three intervals: 15×2^q elements in $R_i < R < 0.1\, R_e$, 5×2^q elements in $0.1\, R_e < R < 0.5\, R_e$, and 4×2^q elements in $0.5\, R_e < R < R_e$. This mesh is similar to the meshes used by Aguiar et al. [8] in computational studies of the disk problem in the context of the linear elasticity theory. The initial guess used in the numerical procedure corresponds to the undistorted reference configuration, which implies that $\mathbf{s}_0 = \mathbf{0}$. In addition, we consider $R_i = 0.001$, $R_e = 1$, $p = 0.1$, and $\varepsilon = 0.1$.

In Fig. 1, we show u_r (top left), ν (top right), $\det \mathbf{F}$ (bottom left), and λ (bottom right) versus the radius R in a neighborhood of the inner surface of the disk. The colored lines correspond to approximate solutions of the nonlinear disk problem using the augmented Lagrangian formulation with increasing mesh refinements, $\delta_f^a = 10^4$, and $d = 1$. Recall from above that d is the degree of the Lagrange finite elements used in the approximation of the displacement field. These colored lines are almost indistinguishable, which indicates the convergence of the numerical results. Using $d = 2$, $\delta_0 = 10^3$, and $\delta_f^p = 10^5$, the numerical results obtained with the penalty formulation are very similar to those shown in Fig. 1. Later in this section, we present a comparison of results obtained with both formulations. The black solid lines correspond to the exact solution of the disk problem in the context of the linear elasticity theory with the imposition of the local injectivity constraint, which is given by the equations (44)-(47) of Aguiar et al. [8].

We see from the graphs of $\det \mathbf{F}$ and λ in Fig. 1 that, in both linear and nonlinear cases, the local injectivity constraint is active in the intervals (R_i, R_a^{lin}) and (R_i, R_a), respectively, where $R_a^{\text{lin}} \approx 0.002$ and $R_a \approx 0.010$. In addition, in (R_i, R_a^{lin}), u_r and, consequently, ν of both solutions coincide. This is expected because the active region includes the inner surface of the disk in both linear and nonlinear cases; therefore, in both cases, the radial displacement $u_r = r - R$ must satisfy the ordinary differential equation $\det \mathbf{F} = \nu\, \tau = r'\, r/R = \varepsilon$ in $\mathcal{B}_=$ and the boundary condition $r(R_i) = R_i$, from which we obtain $r(R) = \sqrt{(R^2 - R_i^2)\, \varepsilon + R_i^2}$ in $\mathcal{B}_=$.

Furthermore, we see from Fig. 1 that, even though the radial displacement u_r is continuous, the radial stretch ν has a jump discontinuity at the interface between $\mathcal{B}_=$ and $\mathcal{B}_>$, which corresponds to $R = R_{\mathcal{S}}$. We have verified

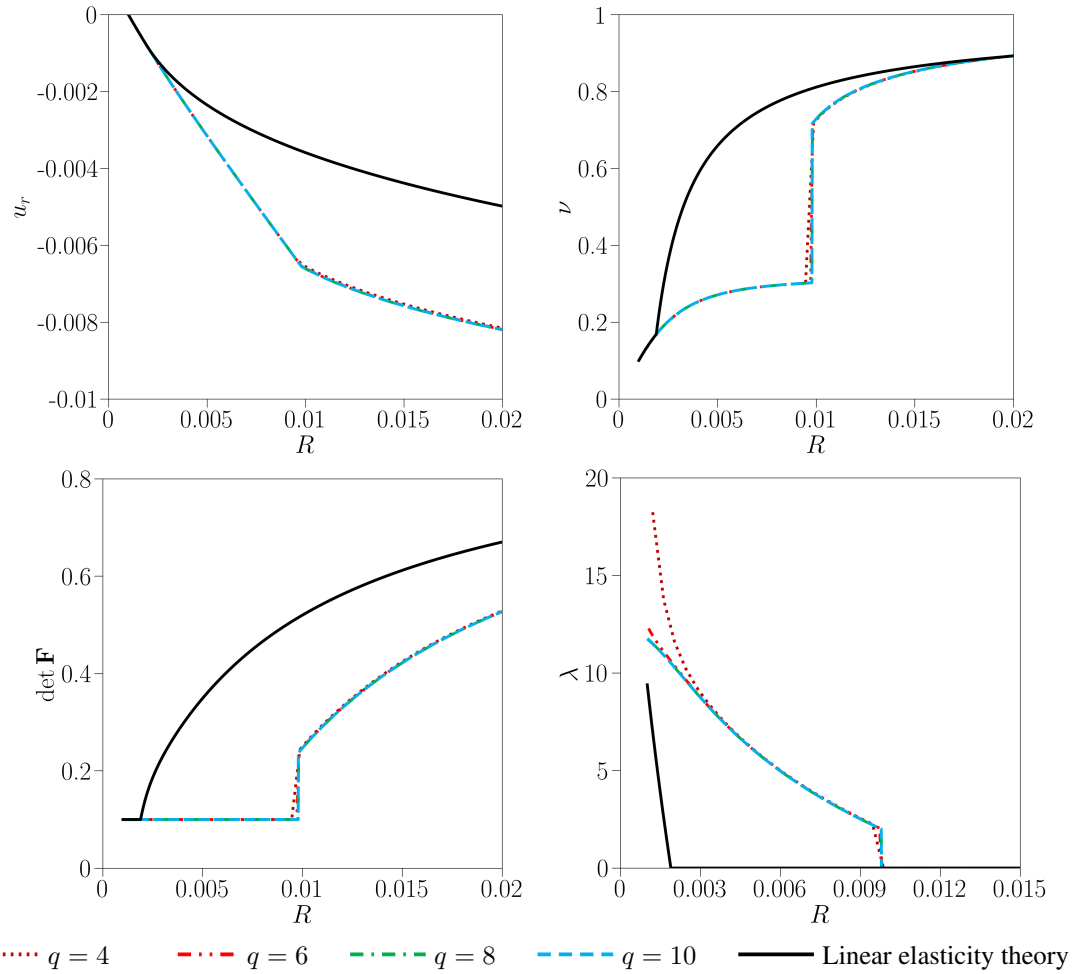

Figure 1. Radial displacement u_r, radial stretch ν, determinant of the deformation gradient $\det \mathbf{F}$, and Lagrange multiplier λ versus the radius R.

that such a jump occurs for $p > \bar{p} = 0.0108$. A similar discontinuity was observed by Aguiar and Rocha [4] and is associated with the non-monotonicity of P_{rr}, given by eq. (8), with respect to ν. In addition, in $\mathcal{B}_=$, the disk is considerably more deformed than in $\mathcal{B}_>$. For radially fiber-reinforced materials, this could indicate that $\bar{p}$ is a critical value of pressure above which, near the inner surface of the disk, the fibers fail by kinking since the surface of discontinuity of the deformation gradient is normal to the fiber direction [9].

We now focus on the comparison between the penalty and augmented Lagrangian formulations. In particular, on how accurately the constraint $\det \mathbf{F} = \varepsilon$ in $\mathcal{B}_=$ is imposed when we use different meshes and finite elements, that is, different values of q and d, respectively. We also study the influence of δ_f^p and δ_f^a on the penalty and augmented Lagrangian formulations, respectively. The results presented below were obtained using the same pressure, disk geometry, and material parameters used in the previous numerical example. In addition, all the results concerning the penalty formulation were obtained using $\delta_0 = 10^3$.

We define the error $e \triangleq \sqrt{\int_{\mathcal{B}_=} (\det \mathbf{F} - \varepsilon)^2 \, \mathrm{d}\mathbf{x}}$ and, in Fig. 2, we plot $\log_{10} e$ versus $\log_{10} \delta_f^p$ and $\log_{10} \delta_f^a$. The two graphs on the top part of the figure refer to results obtained with $d = 1$ and increasing values of q. The two graphs on the bottom part refer to results obtained with $q = 6$ and increasing values of d. The graphs on the left and right sides refer to, respectively, the penalty and the augmented Lagrangian formulations.

We see from the top left graph of Fig. 2 that, in the penalty formulation, e decreases as δ_f^p increases until it reaches a critical value that reduces as q increases. From the top right graph, we see that e decreases as q increases, independently of the value of δ_f^a.

Similarly, we see from the bottom left graph of Fig. 2 that, in the penalty formulation, the error e decreases as δ_f^p increases until it reaches a critical value that reduces as d increases. From the bottom right graph, we see that the augmented Lagrangian formulation has a similar behavior. However, in this case, the critical value is reached with lower values of δ_f^a.

For large enough penalty parameters, we see from Fig. 2 that, in both formulations, an increase of two units

in q, which approximately quadruplicates the number of degrees of freedom, reduces $\log_{10} e$ in approximately 0.6 unit. On the other hand, an increase of one unit in d, which less than duplicates the number of degrees of freedom, reduces $\log_{10} e$ in approximately 2 units. Therefore, our results indicate that, to reduce the error e on the imposition of the injectivity constraint in $B_=$, it is preferable to increase the degree of the finite element approximation than to increase the number of mesh elements.

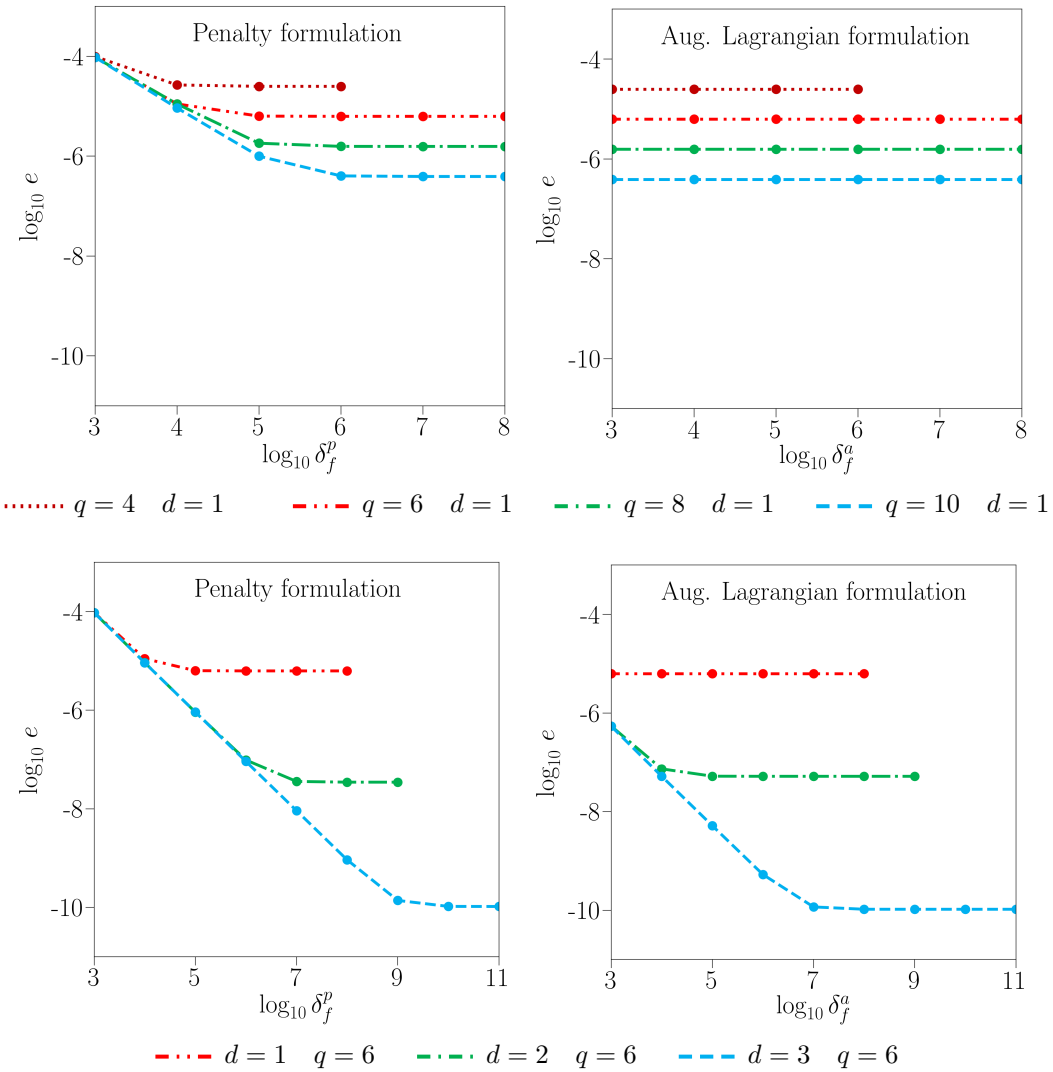

Figure 2. Base 10 logarithm of the error e versus base 10 logarithm of the final penalty parameters δ_f^p and δ_f^a.

4 Conclusions

We have considered the problem of an elastic annular disk in equilibrium in the absence of body force. The disk is fixed on its inner surface and compressed by a uniform pressure on its outer surface. The disk is made of a cylindrically orthotropic material with a nonlinear constitutive response that is stiffer in the radial direction than in the tangential direction. Aguiar and Rocha [4] have found that the solution of this problem predicts material overlapping if the pressure is large enough. To avoid this physically unacceptable behavior, we have formulated the disk problem as a minimization problem of the total potential energy functional with the local injectivity constraint. We have implemented the penalty and the augmented Lagrangian formulations, which have yielded convergent numerical results that do not predict material overlapping. Our results indicate that, to impose the local injectivity constraint accurately, it is preferable to increase the degree of the finite element approximation than to increase the number of finite elements in the mesh. In addition, the solution of the nonlinear disk problem corresponds to a deformation field that has a jump discontinuity in the radial stretch, which delimits a region where the disk is considerably more deformed. For fiber-reinforced materials, this could indicate a region where the fibers failed.

Acknowledgements. The authors acknowledge the support of the National Council for Scientific and Technological Development (CNPq), grant n° 306832/2022-4, São Paulo Research Foundation (FAPESP), grant n° 2022/07083-8, and Coordination for the Improvement of Higher Education Personnel (CAPES) – Finance Code 001.

Authorship statement. The authors hereby confirm that they are the sole liable persons responsible for the authorship of this work, and that all material that has been herein included as part of the present paper is either the property (and authorship) of the authors, or has the permission of the owners to be included here.

References

[1] Forest Products Laboratory. Wood handbook - Wood as an engineering material. Technical report, U.S. Department of Agriculture, Forest Service, Forest Products Laboratory, Madison, 2010.

[2] R. M. Christensen. Properties of carbon fibers. *Journal of the Mechanics and Physics of Solids*, vol. 42, n. 4, pp. 681–695, 1994.

[3] I. M. Daniel and O. Ishai. *Engineering Mechanics of Composite Materials*. Number v. 13 in Engineering mechanics of composite materials. Oxford University Press, New York, 2 edition, 2006.

[4] A. R. Aguiar and L. A. Rocha. Numerical investigation of non-smooth solutions in finite elasticity. In *Proceedings of the 27th International Congress of Mechanical Engineering*. (Accepted for publication), 2023.

[5] R. L. Fosdick and G. Royer-Carfagni. The constraint of local injectivity in linear elasticity theory. *Proceedings of the Royal Society A: Mathematical, Physical and Engineering Sciences*, vol. 457, n. 2013, pp. 2167–2187, 2001.

[6] P. G. Ciarlet. *Mathematical elasticity, volume I: Three-dimensional elasticity*. North-Holand, Amsterdam, 1988.

[7] D. G. Luenberger and Y. Ye. *Linear and Nonlinear Programming*, volume 116 of *International Series in Operations Research & Management Science*. Springer US, New York, NY, 2008.

[8] A. R. Aguiar, R. L. Fosdick, and J. Sanchez. A study of penalty formulations used in the numerical approximation of a radially symmetric elasticity problem. *Journal of Mechanics of Materials and Structures*, vol. 3, n. 8, 2008.

[9] J. Merodio and R. W. Ogden. Material instabilities in fiber-reinforced nonlinearly elastic solids under plane deformation. *Archive of mechanics*, vol. 54, n. 5-6, pp. 525–552, 2002.